CONTROLLING THE TRANSMISSION DYNAMICS OF COVID-19

STEPHEN EDWARD MOORE[1,*], ERIC OKYERE[2]

[1]Department of Mathematics, University of Cape Coast, Ghana

[2]Department of Mathematics and Statistics, University of Energy and Natural Resources, Sunyani, Ghana

Abstract. The outbreak of COVID-19 caused by SARS-CoV-2 in Wuhan and other cities in China in 2019 has become a global pandemic as declared by the World Health Organization (WHO) in the first quarter of 2020. The delay in diagnosis, limited hospital resources and other treatment resources led to the rapid spread of COVID-19. Optimal control dynamical models with time-dependent functions are very powerful mathematical modeling tools to investigate the transmission of infectious diseases. In this study, we have introduced and studied a new mathematical model for COVID-19 disease using personal protection, hospitalization and treatment of infectious individuals with early diagnosis, hospitalization and treatment of infectious individuals with delayed diagnosis and spraying of the environment as time-dependent control functions. This new non-autonomous deterministic epidemic model for the 2019 coronavirus disease is an extension of a recently constructed and analyzed data-driven non-optimal control model. We investigated three control strategies for our model problem. From the numerical illustrations of the various control strategies, we realized that the third strategy, which captures all the four time-dependent control functions, yields better results.

Keywords: COVID-19; delay in diagnosis; dynamic model; compartmental models; optimal control; Hamiltonian.

2010 AMS Subject Classification: 49L20.

---

*Corresponding author

E-mail address: stephen.moore@ucc.edu.gh

1. INTRODUCTION

The recent outbreak of the deadly and highly infectious COVID-19 disease caused by SARS-CoV-2 in Wuhan and other cities in China in 2019 has become a global pandemic as declared by the World Health Organization (WHO) in the first quarter of 2020 [1]. The most vulnerable people to develop serious complications from this dangerous disease are the elderly with underlying medical problems. According to the WHO weekly epidemiological update on COVID-19 released on September 14, 2021, around 4 million new cases were reported worldwide, indicating the first major decline in weekly cases in over two months, see [2].

Recently, several peer-reviewed journal publishers such as Wiley, Elsevier, Hindawi, Springer, Taylor & Francis have made open access to several literature for interested researchers in the epidemiology of COVID-19 disease [3, 4, 5, 6, 7]. The use of mathematical modeling tools and methods to understand the transmission dynamics and control of infectious disease spread, which is usually called mathematical epidemiology, is widely studied and explored [8, 9, 10]. Mathematical modeling of the recent outbreak of the deadly COVID-19 infectious disease has been explored by many authors in the literature, see eg. [11, 12, 13, 14]. An SEIR mathematical model for the transmission dynamics of COVID-19 disease with data fitting, parameter estimations, and sensitivity analysis has been studied in [15] whiles a deterministic model for COVID-19 that captures the effect of delayed diagnosis on the disease transmission has also been presented, see [16]. In [17], the authors explore a statistical analysis of COVID-19 disease data to estimate the time-delay adjusted risk for death from this deadly virus in Wuhan, as well as for China excluding Wuhan. Their study suggested that effective social distancing and movement restriction practices can help minimise disease transmission. A real-time forecast phenomenological model has also been designed to study the transmission pattern of COVID-19 infectious disease, see e.g., [18]. Also, an SEIR-type compartmental modeling concept was applied to design a data-driven epidemic model that incorporates governmental actions and individual behavioral reactions to the COVID-19 disease outbreak in Wuhan [19]. The authors in [20] have developed and examined an SEIR deterministic mathematical model to study the spread dynamics of COVID-19 infections in Indonesia. They

presented global stability analysis for their COVID-19 epidemic model.

The author in [21] has introduced an SIRI COVID-19 epidemic mathematical model to explain how a hypothetical vaccine could affect the transmission dynamics of the disease by incorporating behavior changes of individuals in response to media coverage concerning the disease spread. Some basic epidemiological modeling studies on the COVID-19 pandemic that give useful insight into the dynamics of the infection rate and the recovered rate is presented in [22]. A deterministic SEIR COVID-19 epidemic model with a nonlinear incidence rate that captures government actions is proposed and studied [23]. A mathematical model based on epidemic modelling conceptual framework with data-driven dynamics is formulated and analysed to explore the role of individuals and governmental reactions on the transmission dynamics of COVID-19 [24]. An SEIR-type nonlinear COVID-19 epidemiological model that captures quarantine, asymptomatic, and isolation compartments in the modelling framework is constructed and studied using standard incidence rate [25]. Using an SEIR compartmental modeling approach and the reported cases of COVID-19 in the Hubei province, the authors in [26] applied the particle swarm optimization algorithm to estimate their model parameters.

Mathematical modelling of epidemics using deterministic optimal control problems is widely explored in the literature of mathematical epidemiology. A detailed comprehensive literature of optimal control models in epidemiological modeling and numerical approximation techniques can be found in [27, 28]. Several works in the literature reveal that epidemic models that are constructed with optimal control problems are appropriate and very useful for suggesting control strategies to curb disease spread, see, e.g., [29, 30, 31, 32, 33].

In this article, we present and analyze control strategies to examine the transmission dynamics of the 2019 highly infectious coronavirus disease and to determine strategies that are critical even during instances of delay in diagnosis. The deterministic model of our control model has recently been considered by [16], where they presented data-driven simulations.

The rest of the article is organized as follows: In Section 2, we formulate an optimal control model for COVID-19 with four control measures. In Section 3, we present the numerical results of the optimal control model. Finally, we conclude in Section 4 with discussions on the control measures.

2. FORMULATION OF THE OPTIMAL CONTROL PROBLEM

In this section, we formulate an optimal control model for COVID-19 to derive four control measures with minimal implementation cost to eradicate the disease after a defined period of time. The deterministic model was introduced in [16] as follows. The population is divided into susceptible $(S(t))$, self-quarantine susceptible $(S_q(t))$, exposed $(E(t))$, infectious with timely diagnosis $(I_1(t))$, infectious with delayed diagnosis $(I_2(t))$ usually as a result limited diagnostic tools or hospitals, hospitalized $(H(t))$, recovered $(R(t))$ and the viral spread in the environment $(V(t))$. Hence for the total human population at time t we have $N = S(t) + S_q(t) + E(t) + I_1(t) + I_2(t) + H(t) + R(t)$. Following the compartmental transition diagram as shown in Figure 1, the eight-state dynamical model describing the transmission dynamics of COVID-19 is given by
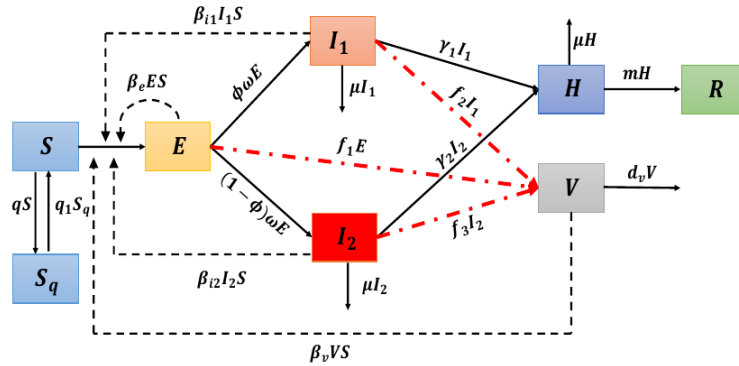
FIGURE 1. Compartmental diagram for the transmission dynamics of COVID-19, see also [16].

$$\frac{dS}{dt} = -(\beta_e E + \beta_{i_1} I_1 + \beta_{i_2} I_2 + \beta_v V)S - qS + q_1 S_q$$

$$\frac{dS_q}{dt} = qS - q_1 S_q$$

$$\frac{dE}{dt} = (\beta_e E + \beta_{i_1} I_1 + \beta_{i_2} I_2 + \beta_v V)S - \omega E$$

(1)

$$\frac{dI_1}{dt} = \phi \omega E - \gamma_1 I_1 - \mu I_1$$

$$\frac{dI_2}{dt} = (1-\phi)\omega E - \gamma_2 I_2 - \mu I_2$$

$$\frac{dH}{dt} = \gamma_1 I_1 + \gamma_2 I_2 - mH - \mu H$$

$$\frac{dR}{dt} = mH$$

$$\frac{dV}{dt} = f_1 E + f_2 I_1 + f_3 I_2 - d_v V,$$

where $S(0) \geq 0, S_q(0) \geq 0, E(0) \geq 0, I_1(0) \geq 0, I_2(0) \geq 0, H(0) \geq 0, R(0) \geq 0$ and $V(0) \geq 0$.

The description of the parameters used in the model for the COVID-19 transmission are given in Table 1.

TABLE 1. Description of parameters.

Parameter	Description
q	Self-quarantined rate of the susceptible
q_1	Transition rate of self-quarantined individuals to the susceptible
β_e	Transmission rate from the exposed to the susceptible
β_{i_1}	Transmission rate from the infectious with timely diagnosis to the susceptible
β_{i_2}	Transmission rate from the infectious with delayed diagnosis to the susceptible
β_v	Transmission rate from the susceptible to the exposed (infected by virus)
$1/\omega$	Incubation period
ϕ	Proportion of the infectious with timely diagnosis
$1/\gamma_1$	Waiting time of the infectious for timely diagnosis
$1/\gamma_2$	Waiting time of the infectious for delayed diagnosis
μ	Disease-induced death rate
m	Recovery rate of the hospitalized
f_1	Virus released rate of the exposed
f_2	Virus released rate of the infectious with timely-diagnosis
f_3	Virus released rate of the infectious with delayed-diagnosis
d_v	Decay rate of virus in the environment

2.1. COVID-19 Model Problem with Control Measures. Following from the system (1), we modified the transmission rate by reducing the factor by $(1 - u_1(t))$, where $u_1(t)$ measures the effort of individuals to protect themselves (i.e. personal protection). The control variable $u_2(t)$ measures the treatment rate of timely diagnosed individuals whiles the $u_3(t)$ measures the treatment rate of delayed diagnosed individuals. We assume that $u_2(t)I_1$ and $u_3(t)I_2$ individuals are removed from the timely diagnosed class and delayed diagnosed class and added to the Hospitalized class. The fourth control variable $u_4(t)$ measures the spraying of the environment to prevent viral release. We also assume that $u_4(t)V$ virus are removed from the environment. We further assume that individuals that recovers at any time t after hospitalization and treatment are removed from the hospitalized class to the recovered class. Therefore, we seek to minimize a time-dependent functional given by

$$(2) \qquad \mathscr{J}(u_1, u_2, u_3, u_4) := \min \int_0^T \left(A_1 E(t) + A_2 I_2(t) + A_3 V(t) + \frac{1}{2} \sum_{i=1}^4 C_i u_i^2(t) \right) dt.$$

subject to the constraint

$$
\begin{aligned}
\frac{dS}{dt} &= -(1 - u_1(t))(\beta_e E(t) + \beta_{i_1} I_1(t) + \beta_{i_2} I_2(t) + \beta_v V(t))S(t) - qS(t) + q_1 S_q(t) \\
\frac{dS_q}{dt} &= qS(t) - q_1 S_q(t) \\
\frac{dE}{dt} &= (1 - u_1(t))(\beta_e E(t) + \beta_{i_1} I_1(t) + \beta_{i_2} I_2(t) + \beta_v V(t))S(t) - \omega E(t) \\
(3) \qquad \frac{dI_1}{dt} &= \phi \omega E(t) - u_2(t) I_1(t) - \mu I_1(t) \\
\frac{dI_2}{dt} &= (1 - \phi)\omega E(t) - u_3(t) I_2(t) - \mu I_2(t) \\
\frac{dH}{dt} &= u_2(t) I_1(t) + u_3(t) I_2(t) - mH(t) - \mu H(t) \\
\frac{dR}{dt} &= mH(t) \\
\frac{dV}{dt} &= f_1 E(t) + f_2 I_1(t) + f_3 I_2(t) - d_v V(t) - u_4(t)V,
\end{aligned}
$$

All the control efforts $u_i(t), i = 1, \ldots, 4$ are assumed to be bounded and Lebesgue measurable time-dependent functions on the interval $[0, T]$ where T is the final time and where the

admissible control set is defined as

$$(4) \qquad \mathscr{U} := \{u_i(t) \mid \quad 0 \le u_i(t) \le 1, t \in [0,T] \quad \text{for} \quad i = 1,\dots,4\},$$

The weight constants A_1, A_2 and A_3 are associated with exposed individuals, infectious individuals with delayed diagnosis and the environment respectively whiles the weights C_1, C_2, C_3 and C_4 are the balancing cost factors associated with the time-dependent control functions $u_1(t), u_2(t), u_3(t)$ and $u_4(t)$ respectively.

In the next section, we prove the existence of an optimal control for the system (3) and then derive the optimality system. It is well known that Pontryagin's maximum principle (PMP) is required to solve this control problem and the derivation of the necessary conditions [34, 35].

2.2. Existence of an Optimal Control.
The necessary conditions include the optimality solutions and the adjoint equations that an optimal control must satisfy which come from Pontryagin's maximum principle [35]. This principle converts the control model (3) and the objective functional (2) into a problem of minimizing pointwise Hamiltonian function (6), which is formed by allowing each of the adjoint variables to correspond to each of the state variables accordingly and combining the results with the objective functional.

Theorem 1. *Given the objective functional $\mathscr{J}(u_1, u_2, u_3, u_4)$ as in (2), where the control set $\mathscr{U}$ given by (4) is measurable subject to (3) with initial conditions given at $t = 0$, then there exists an optimal control $u^* = (u_1^*(t), u_2^*(t), u_3^*(t), u_4^*(t))$ such that*

$$\mathscr{J}(u_1^*(t), u_2^*(t), u_3^*(t), u_4^*(t)) := \min\{\mathscr{J}(u_1, u_2, u_3, u_4), (u_1, u_2, u_3, u_4) \in \mathscr{U}\}.$$

Proof. The existence of an optimal control due to the convexity of the integrand of $\mathscr{J}$ with respect to the control measures $u_i(t), i = 1,\dots,4$, an *a priori* boundedness of the solutions of both the state and adjoint equations and the Lipchitz property of the state system with respect to the state variables follows from [36]. $\qquad \square$

To find the optimal solution, we need the Lagrangian ($\mathbf{L}$) and Hamiltonian ($\mathbf{H}$) for the optimal control problem (3) and (2). The Lagrangian of the control problem is given by

$$(5) \qquad \mathbf{L} := A_1 E(t) + A_2 I_2(t) + + A_3 V(t) + \frac{1}{2} \sum_{i=1}^{4} C_i u_i^2(t).$$

Since we want the minimal value of the Lagrangian, we define the Hamiltonian function for the system as

(6)

$$\mathbf{H} = A_1 E(t) + A_2 I_2(t) + A_3 V(t) + \frac{1}{2}\left(C_1 u_1^2(t) + C_2 u_2^2(t) + C_3 u_3^2(t) + C_4 u_4^2(t) \right)$$

$$+ \lambda_S \left[-(1 - u_1(t))(\beta_e E(t) + \beta_{i_1} I_1(t) + \beta_{i_2} I_2(t) + \beta_v V(t)) S(t) - q S(t) + q_1 S_q(t) \right]$$

$$+ \lambda_{S_q} \left[q S(t) - q_1 S_q(t) \right] + \lambda_E \left[(1 - u_1(t))(\beta_e E(t) + \beta_{i_1} I_1(t) + \beta_{i_2} I_2(t) + \beta_v V(t)) S(t) - w E(t) \right]$$

$$+ \lambda_{I_1} \left[\phi w E(t) - u_2(t) I_1(t) - \mu I_1(t) \right] + \lambda_{I_2} \left[(1 - \phi) w E(t) - u_3(t) I_2(t) - \mu I_2(t) \right]$$

$$+ \lambda_H \left[u_2(t) I_1(t) + u_3(t) I_2(t) - m H(t) - \mu H(t) \right]$$

$$+ \lambda_R m H(t) + \lambda_V \left[f_1 E(t) + f_2 I_1(t) + f_3 I_2(t) - d_v V(t) - u_4(t) V(t) \right].$$

where $\lambda_j, j \in \{S, S_q, E, I_1, I_2, H, R, V\}$ are the adjoint variables.

Following the popularly known Pontryagin Maximum Principle [35], we determine an optimal solution for a given optimal control problem as follows; Suppose that (ξ, φ) represent an optimal control solution for a given dynamical optimal control problem, then there exist adjoint or co-state variables, $\omega = (\omega_1, \omega_2, \cdots, \omega_n)$ which satisfies the equation below

$$(7) \qquad \frac{d\xi}{dt} = \frac{\partial \mathbf{H}(t, \xi, \varphi, \omega)}{\partial \omega}, \quad 0 = \frac{\partial \mathbf{H}(t, \xi, \varphi, \omega)}{\partial \varphi}, \text{ and } \quad \frac{d\omega}{dt} = -\frac{\partial \mathbf{H}(t, \xi, \varphi, \omega)}{\partial \xi}.$$

Then by applying equation (7) and the formulated Hamiltonian function (6), the adjoint or co-state state system and the optimal control characterisation for our constructed optimal control dynamical model are given in the following theorem.

Theorem 2. *Let* $(u_1{}^*, u_2{}^*, u_3{}^*, u_4{}^*)$ *be an optimal control and suppose that* $(S^*, S_q{}^*, E^*, I_1{}^*, I_2{}^*, H^*, R^*, V^*)$ *is an optimal control solution for the dynamical optimal control*

problem (2)-(3) that minimize $\mathscr{J}(u_1,u_2,u_3,u_4)$ over $\mathscr{U}$, then there exist co-state or adjoint variables $\lambda_S, \lambda_{S_q}, \lambda_{I_1}, \lambda_{I_2}, \lambda_H, \lambda_R$ and λ_V that satisfies the system below

$$
\begin{aligned}
\frac{d\lambda_S}{dt} &= (\lambda_S - \lambda_E)(1 - u_1^*(t))\left[\beta_e E^*(t) + \beta_{i_1} I_1^*(t) + \beta_{i_2} I_2^*(t) + \beta_v V^*(t)\right] + q(\lambda_S - \lambda_E) \\
\frac{d\lambda_{S_q}}{dt} &= q_1(\lambda_{S_q} - \lambda_S) \\
\frac{d\lambda_E}{dt} &= -A_1 + (\lambda_S - \lambda_E)(1 - u_1^*(t))\beta_e S^*(t) + w\lambda_E - \phi w \lambda_{I_1} - (1 - \phi)w\lambda_{I_2} - f_1 \lambda_V \\
\frac{d\lambda_{I_1}}{dt} &= (\lambda_S - \lambda_E)(1 - u_1^*(t))\beta_{i_1} S^*(t) + (\lambda_{I_1} - \lambda_H)u_2^*(t) + \lambda_{I_1}\mu - f_2 \lambda_V \\
\frac{d\lambda_{I_2}}{dt} &= -A_2 + (\lambda_S - \lambda_E)(1 - u_1^*(t))\beta_{i_2} S^*(t) + (\lambda_{I_2} - \lambda_H)u_3^*(t) + \lambda_{I_2}\mu - f_3 \lambda_V \\
\frac{d\lambda_H}{dt} &= m(\lambda_H - \lambda_R) + \mu\lambda_H \\
\frac{d\lambda_R}{dt} &= 0 \\
\frac{d\lambda_V}{dt} &= -A_3 + (\lambda_S - \lambda_E)(1 - u_1^*(t))\beta_v S^*(t) + \lambda_V(d_v + u_4^*(t))
\end{aligned}
\tag{8}
$$

with transversality conditions

$$
\lambda_j(T) = 0, \quad j \in \{S, S_q, E, I_1, I_2, H, R, V\}. \tag{9}
$$

and the control functions u_1^*, u_2^*, u_3^* and u_4^* satisfies the optimality condition given by

$$
\begin{cases}
u_1^*(t) &= \min\{1, \max\{0, \Lambda_1\}\}, \\
u_2^*(t) &= \min\{1, \max\{0, \Lambda_2\}\}, \\
u_3^*(t) &= \min\{1, \max\{0, \Lambda_3\}\}, \\
u_4^*(t) &= \min\{1, \max\{0, \Lambda_4\}\},
\end{cases}
\tag{10}
$$

where

$$
\Lambda_1 = \frac{\left(\lambda_E - \lambda_S\right)(\beta_e E^*(t) + \beta_{i_1} I_1^*(t) + \beta_{i_2} I_2^*(t) + \beta_v V^*(t))S^*(t)}{C_1},
$$

$$
\Lambda_2 = \frac{\left(\lambda_{I_1} - \lambda_H\right)I_1^*(t)}{C_2}, \quad \Lambda_3 = \frac{\left(\lambda_{I_2} - \lambda_H\right)I_2^*(t)}{C_3} \quad and \quad \Lambda_4 = \frac{\lambda_V V^*(t)}{C_4}. \tag{11}
$$

Proof. To deduce the dynamical co-state or adjoint system and the transversality conditions, we apply the well-known Maximum Principle studied in [35] and the constructed Hamiltonian function (6) as follows

$$
(12) \quad
\begin{cases}
\dfrac{d\lambda_S}{dt} = -\dfrac{\partial \mathbf{H}}{\partial S}, \\[2ex]
\dfrac{d\lambda_{S_q}}{dt} = -\dfrac{\partial \mathbf{H}}{\partial S_q}, \\[2ex]
\dfrac{d\lambda_E}{dt} = -\dfrac{\partial \mathbf{H}}{\partial E} \\[2ex]
\dfrac{d\lambda_{I_1}}{dt} = -\dfrac{\partial \mathbf{H}}{\partial I_1},
\end{cases}
\qquad
\begin{cases}
\dfrac{d\lambda_{I_2}}{dt} = -\dfrac{\partial \mathbf{H}}{\partial I_2}, \\[2ex]
\dfrac{d\lambda_H}{dt} = -\dfrac{\partial \mathbf{H}}{\partial H}, \\[2ex]
\dfrac{d\lambda_R}{dt} = -\dfrac{\partial \mathbf{H}}{\partial R}, \\[2ex]
\dfrac{d\lambda_V}{dt} = -\dfrac{\partial \mathbf{H}}{\partial V}.
\end{cases}
$$

with

$$
(13) \qquad \lambda_j(T) = 0, \quad j \in \{S, S_q, E, I_1, I_2, H, R, V\}.
$$

Finally, knowing that on the interior of the control set $\mathscr{U}$, we have

$$
(14) \qquad \frac{\partial \mathbf{H}}{\partial u_1} = 0, \quad \frac{\partial \mathbf{H}}{\partial u_2} = 0, \quad \frac{\partial \mathbf{H}}{\partial u_2} = 0, \quad \frac{\partial \mathbf{H}}{\partial u_3} = 0, \quad \text{and} \quad \frac{\partial \mathbf{H}}{\partial u_4} = 0.
$$

Solving equation (14) for u_1^*, u_2^*, u_3^* and u_4^* yields the control characterization (10). □

3. NUMERICAL RESULTS OF THE OPTIMAL CONTROL ANALYSIS

This section of the study is concerned with numerical solutions for the constructed optimality system using an iterative fourth-order Runge-Kutta with a forward-backward sweep method that is very efficient, useful, and reliable. This useful iterative scheme has widely been applied by several authors who are interested in optimal control modeling in solving their dynamical optimality systems, see, e.g. [37, 38, 39, 32, 31]. The details of this scheme can be found in the monograph [27]. We considered the initial conditions: $S(0) = 11081000$, $S_q(0) = 159$, $E(0) = 399$, $I_1(0) = 28$, $I_2(0) = 54$, $H(0) = 41$, $R(0) = 12$ and $V(0) = 2108$ in [16]. Parameter values required for simulations are also adapted from the same work [16]. We have further assumed

$A_1 = 5, A_2 = 5, A_3 = 10, C_1 = 10, C_2 = 30, C_3 = 25$ and $C_4 = 30$. Figure 2 shows the profiles of the optimal control functions (u_1, u_2, u_3, u_4).
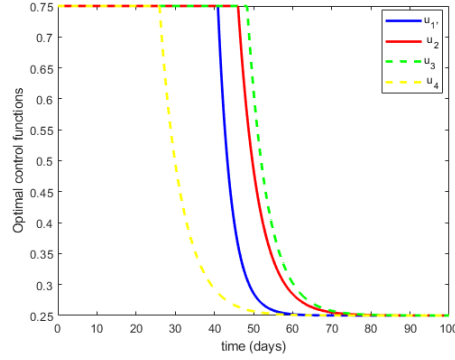
FIGURE 2. Optimal control functions

3.1. Control Strategy I. In this strategy, we consider personal protection $(u_1 \neq 0)$, hospitalization and treatment of infectious individuals with early diagnosis $(u_2 \neq 0)$, hospitalization and treatment of infectious individuals with delay diagnosis, $(u_3 \neq 0)$ as time-dependent control functions to minimise our objective functional. Our main aim in this control strategy is to minimise the number of exposed (E), infectious individuals with delayed diagnosis (I_2) and the virus in the environment (V). In the non-optimal control model (3), hospitalization and treatment of infectious individuals with early diagnosis $(\gamma_1 = u_2 = \frac{1}{2.9})$, and hospitalization and treatment of infectious individuals with delayed diagnosis $(\gamma_2 = u_3 = \frac{1}{10})$ are captured as constant controls, see Figures 3 – 5.
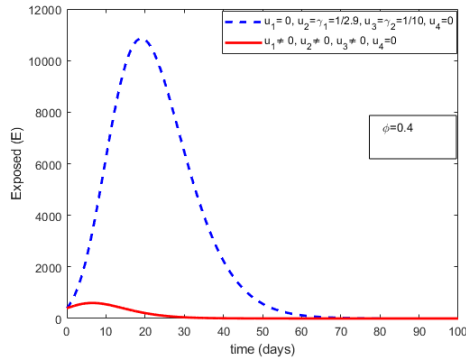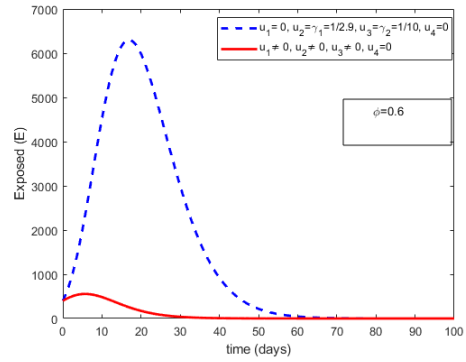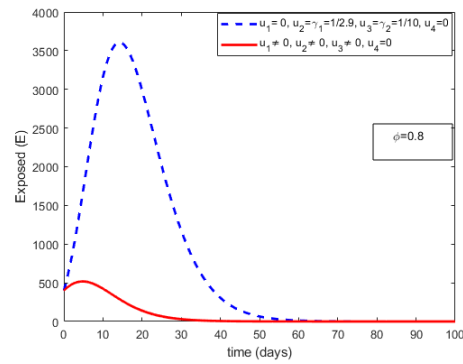
FIGURE 3. Solution trajectories for Exposed individuals with varying parameter $\phi = 0.4$, $\phi = 0.6$ and $\phi = 0.8$. The red line represents the controlled Exposed population, whiles the blue line represents the uncontrolled exposed population.
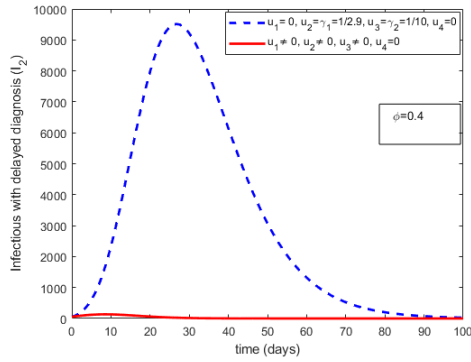
(a)
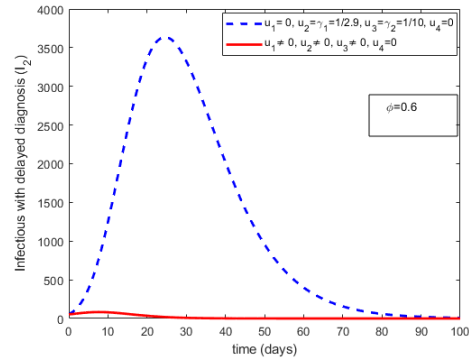
(b)
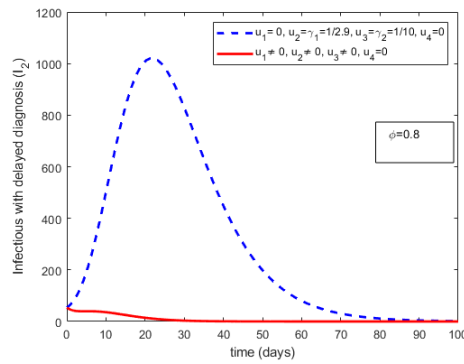
(c)

FIGURE 4. Solution trajectories for Infectious individuals with delayed diagnosis with varying parameter $\phi = 0.4$, $\phi = 0.6$ and $\phi = 0.8$. The red line represents the controlled delayed diagnosed infectious population whiles the blue line represents the uncontrolled infectious population.
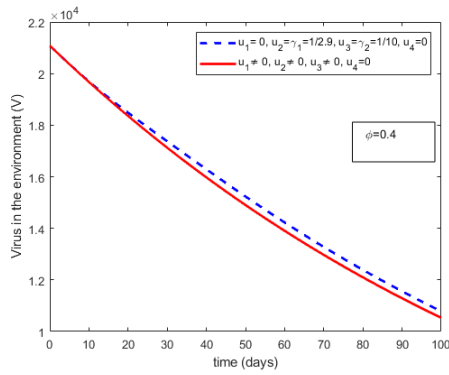
(a)
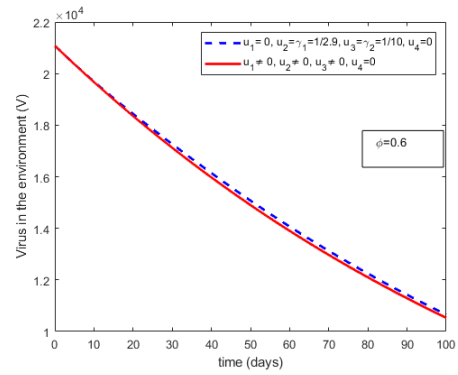
(b)
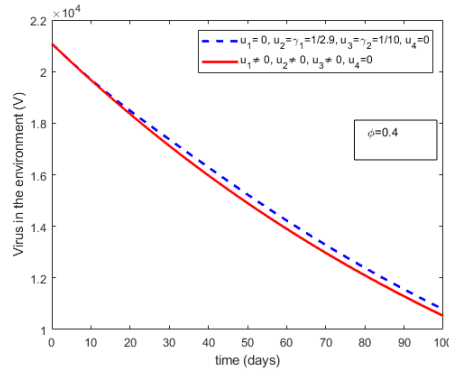
(c)

FIGURE 5. Controlling the viral spread in the environment with varying proportion of sympomatic individuals $\phi = 0.4$, $\phi = 0.6$ and $\phi = 0.8$ where the red line represents the controlled envrionment and the blue line represents the uncontrolled environment.

3.2. Control Strategy II. This strategy deals with hospitalization and treatment of infectious individuals with early diagnosis, $(u_2 \neq 0)$ and hospitalization and treatment of infectious individuals with delayed diagnosis $(u_3 \neq 0)$ to minimise our objective functional. Here, we aim to minimise the number of exposed (E), infectious with delay diagnosis (I_2) and virus in the environment (V). In the non-optimal control model (3), hospitalization and treatment of infectious individuals with early diagnosis $(\gamma_1 = u_2 = \frac{1}{2.9})$ and hospitalization and treatment of infectious individuals with delay diagnosis $(\gamma_2 = u_3 = \frac{1}{10})$ are captured as constant controls, see Figures 6-8.

(a)

(b)

(c)
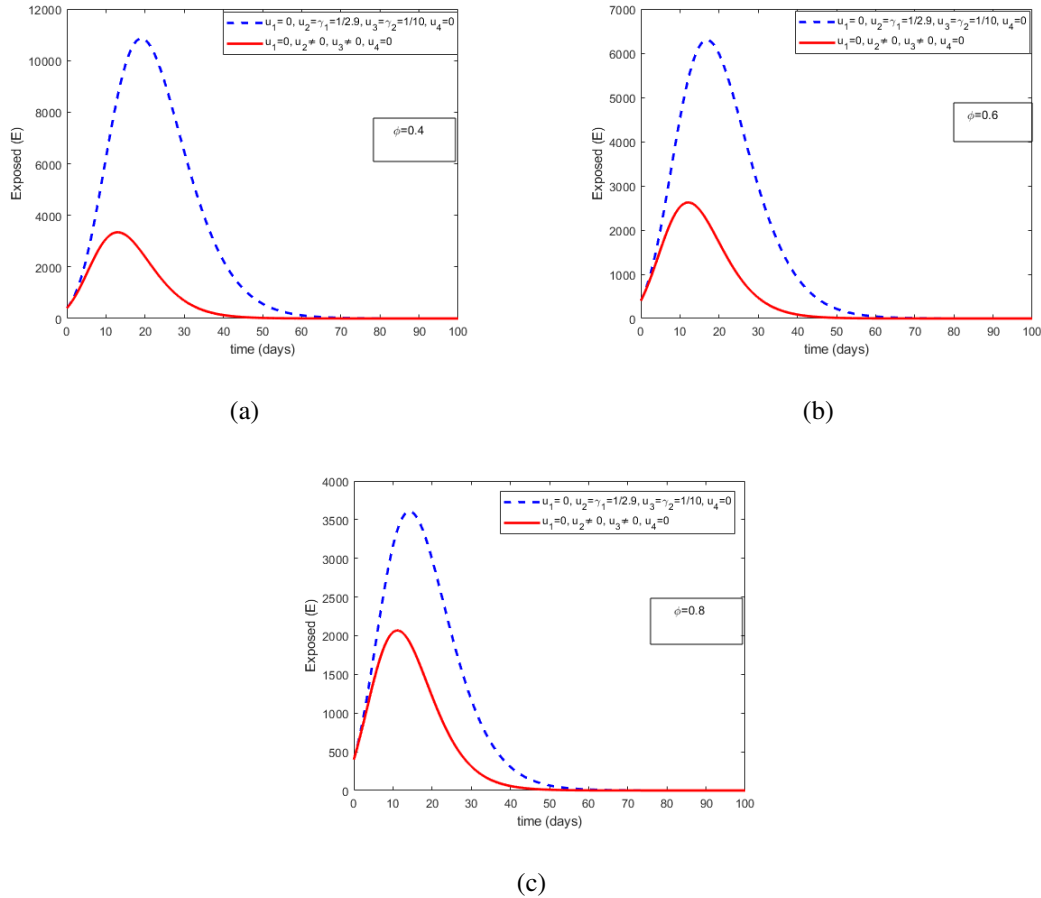
FIGURE 6. Solution trajectories for Exposed individuals with varying parameter $\phi = 0.4$, $\phi = 0.6$ and $\phi = 0.8$. The red line represents the controlled exposed population whiles the blue line represents the uncontrolled exposed population.
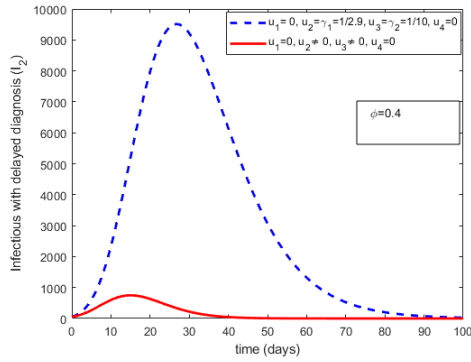
(a)
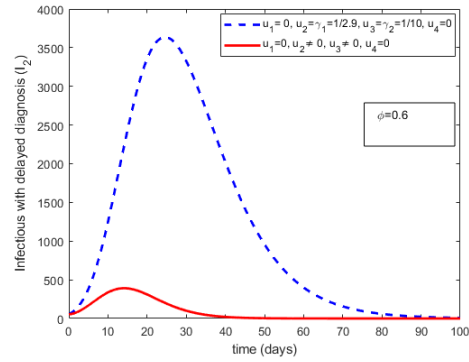
(b)
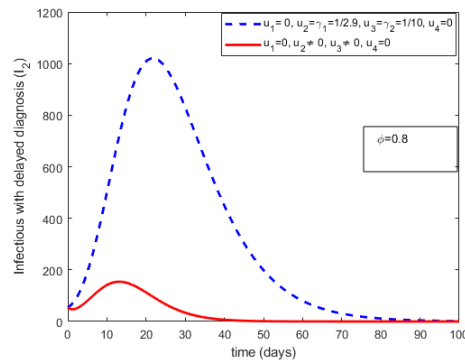
(c)

FIGURE 7. Solution trajectories for Infectious individuals with delayed diagnosis with varying parameter $\phi = 0.4$, $\phi = 0.6$ and $\phi = 0.8$. The red line represents the controlled delayed diagnosed infectious population whiles the blue line represents the uncontrolled infectious population.
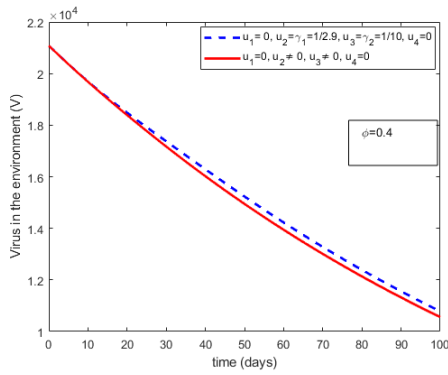
(a)
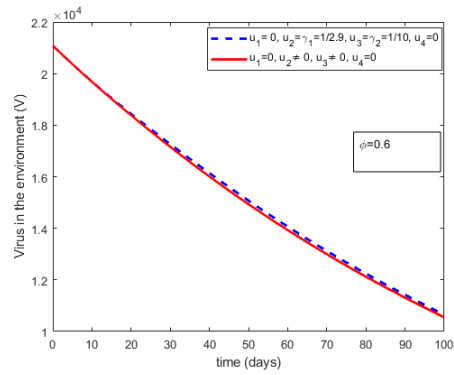
(b)
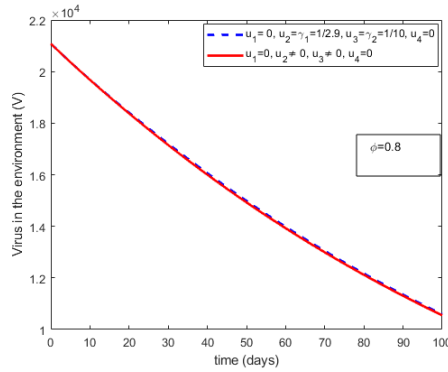
(c)

FIGURE 8. Controlling the viral spread in the environment with varying proportion of symptomatic individuals $\phi = 0.4$, $\phi = 0.6$ and $\phi = 0.8$ where the red line represents the controlled environment and the blue line represents the uncontrolled environment.

3.3. Control Strategy III. In this strategy as presented in Figures 9-11, all the four time-dependent control functions $(u_1 \neq 0, u_2 \neq 0, u_3 \neq 0, u_4 \neq 0)$ proposed in this study are incorporated into the optimal control COVID-19 model problem to minimise the objective function. In the non-optimal control model, treatment with early diagnosis $(\gamma_1 = u_2 = \frac{1}{2.9})$ and treatment with delay diagnosis $(\gamma_2 = u_3 = \frac{1}{10})$ are captured as constant controls.

(a)   (b)

(c)
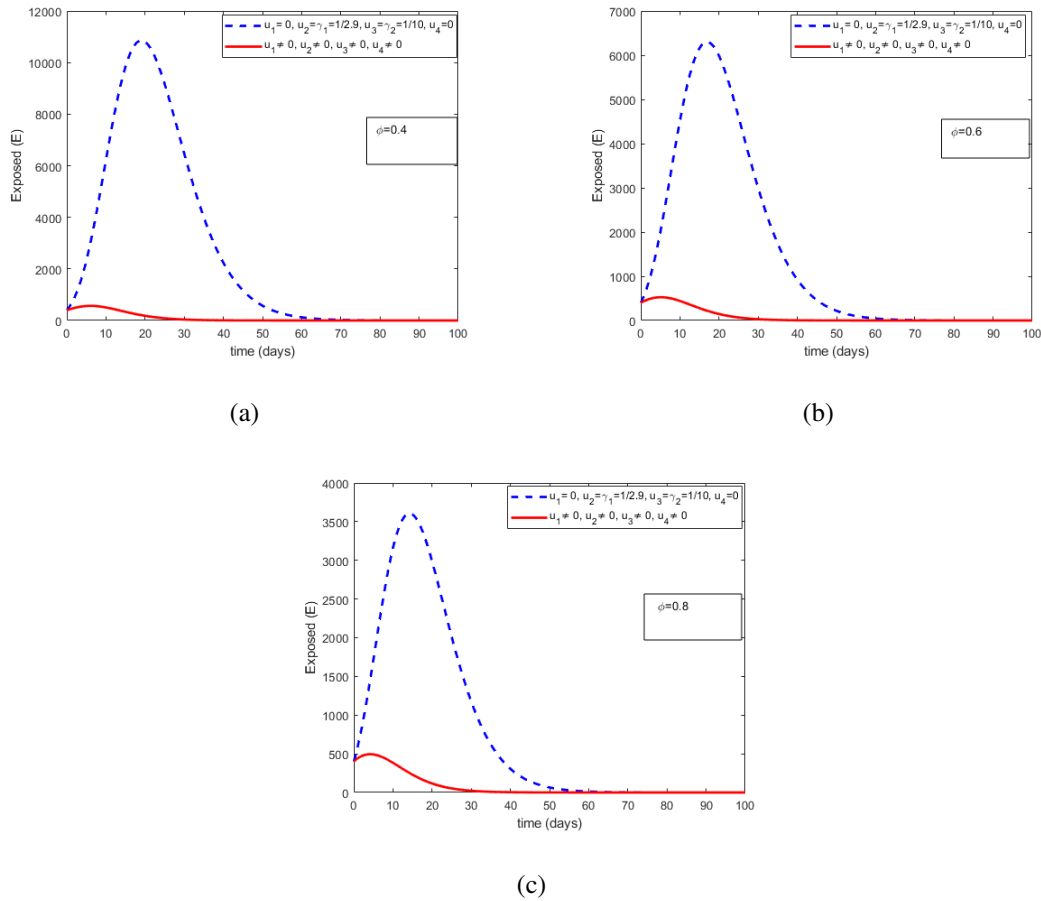
FIGURE 9. Solution trajectories for Exposed individuals with varying parameter $\phi = 0.4$, $\phi = 0.6$ and $\phi = 0.8$. The red line represents the controlled Exposed population whiles the blue line represents the uncontrolled exposed population.
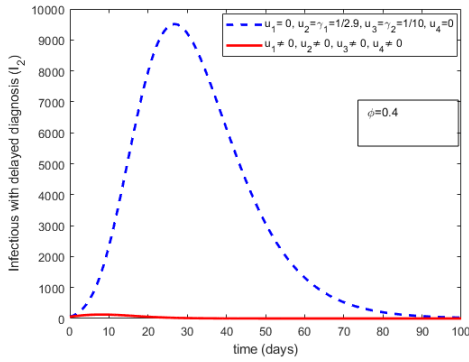
(a)
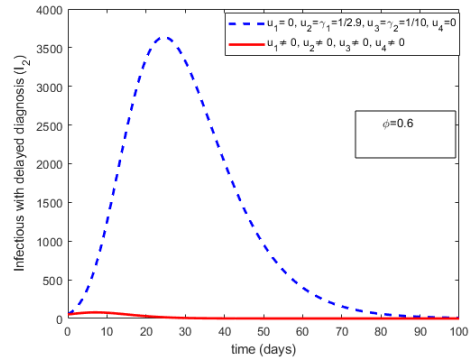
(b)
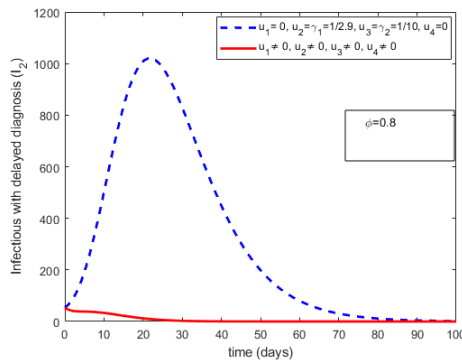
(c)

FIGURE 10. Solution trajectories for Infectious individuals with delayed diagnosis with varying parameter $\phi = 0.4$, $\phi = 0.6$ and $\phi = 0.8$. The red line represents the controlled delayed diagnosed infectious population whiles the blue line represents the uncontrolled infectious population.
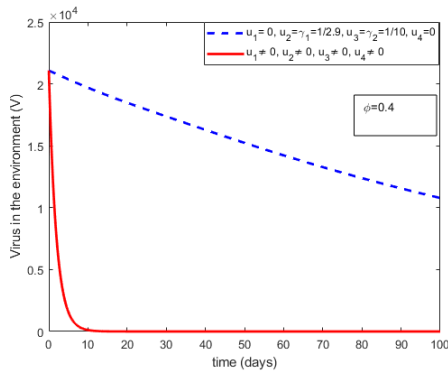
(a)
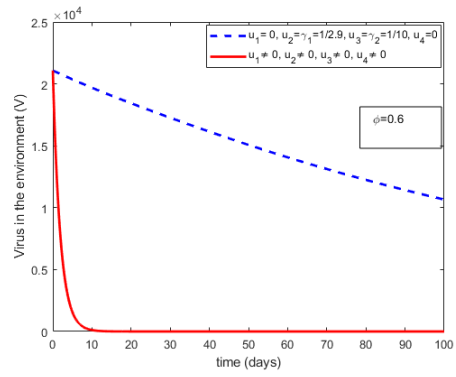
(b)
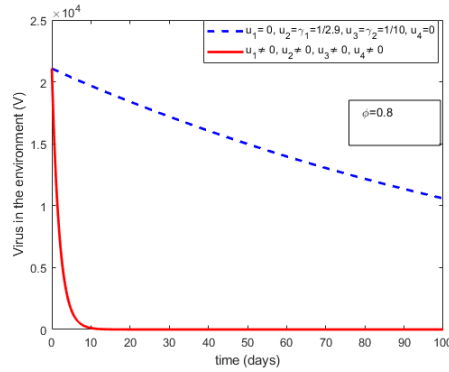
(c)

FIGURE 11. Controlling the viral spread in the environment with varying proportion of symptomatic individuals $\phi = 0.4$, $\phi = 0.6$ and $\phi = 0.8$ where the red line represents the controlled environment and the blue line represents the uncontrolled environment.

3.4. Simulations results for all three optimal control strategies. In this subsection, solution trajectories for the number of exposed, infectious with delay diagnosis and virus in the environment for all the three control strategies are numerically compared with that of the non-optimal control model, see Figures 12-14. Our numerical results suggest that, if people can adhere to effective personal protection practices such as the use of hand sanitizers, washing of hands regularly and social distancing, there will be fewer infections in the population. From our results, we can further argue that, effective spraying of the environment and early diagnosis of infected or infectious individuals and treatment can help reduce the number of COVID-19 infections significantly.

(a)

(b)

(c)
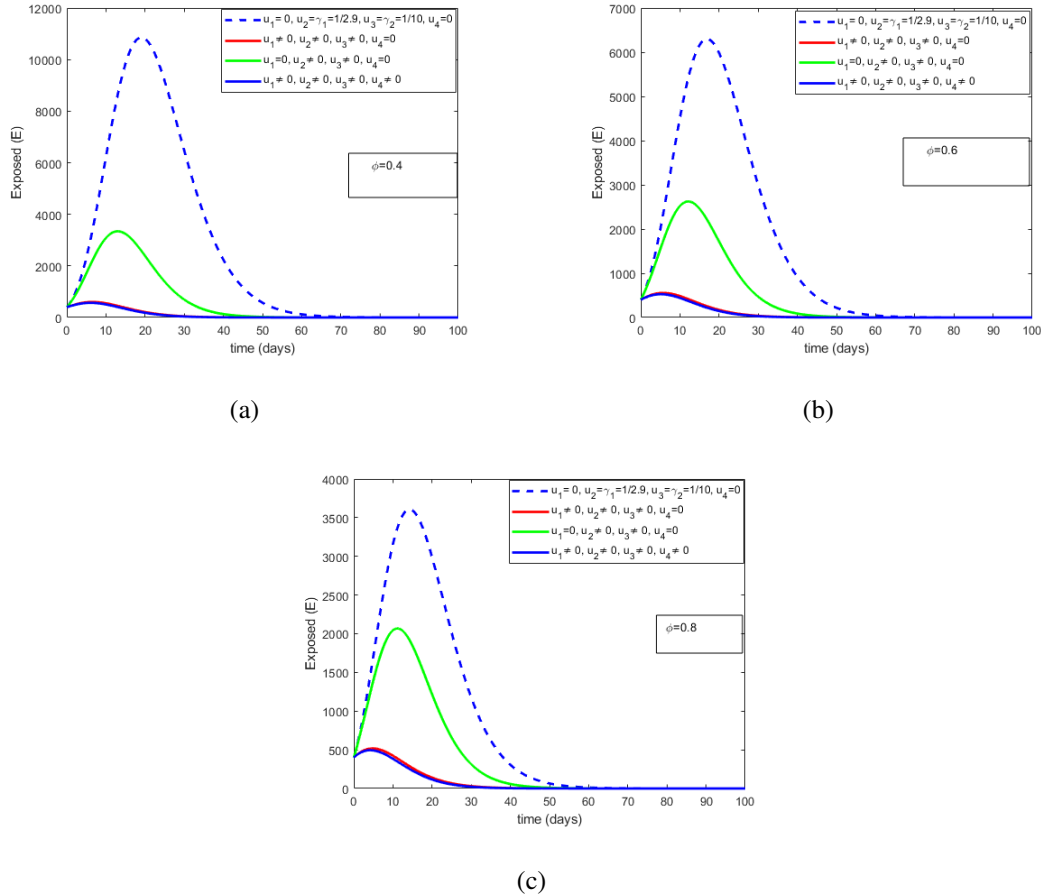
FIGURE 12. Solutions trajectories for Exposed individuals with $\phi = 0.4$, $\phi = 0.6$ and $\phi = 0.8$.
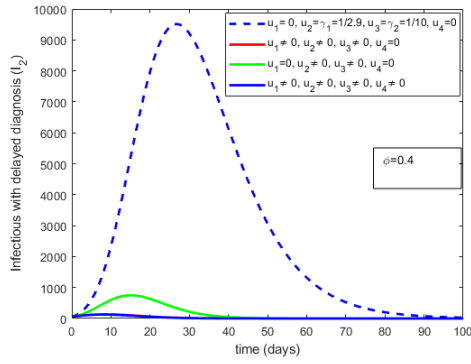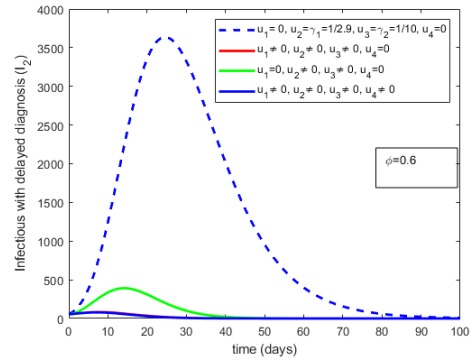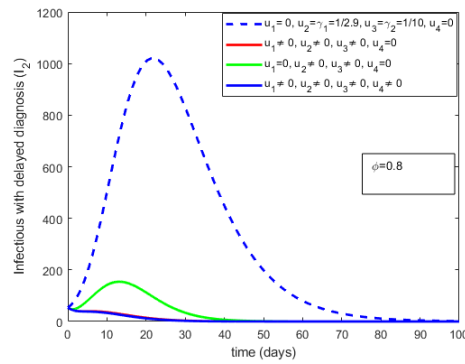
FIGURE 13. Solutions trajectories for Infectious individuals delayed diagnosis with $\phi = 0.4$, $\phi = 0.6$ and $\phi = 0.8$.

(a)

(b)

(c)
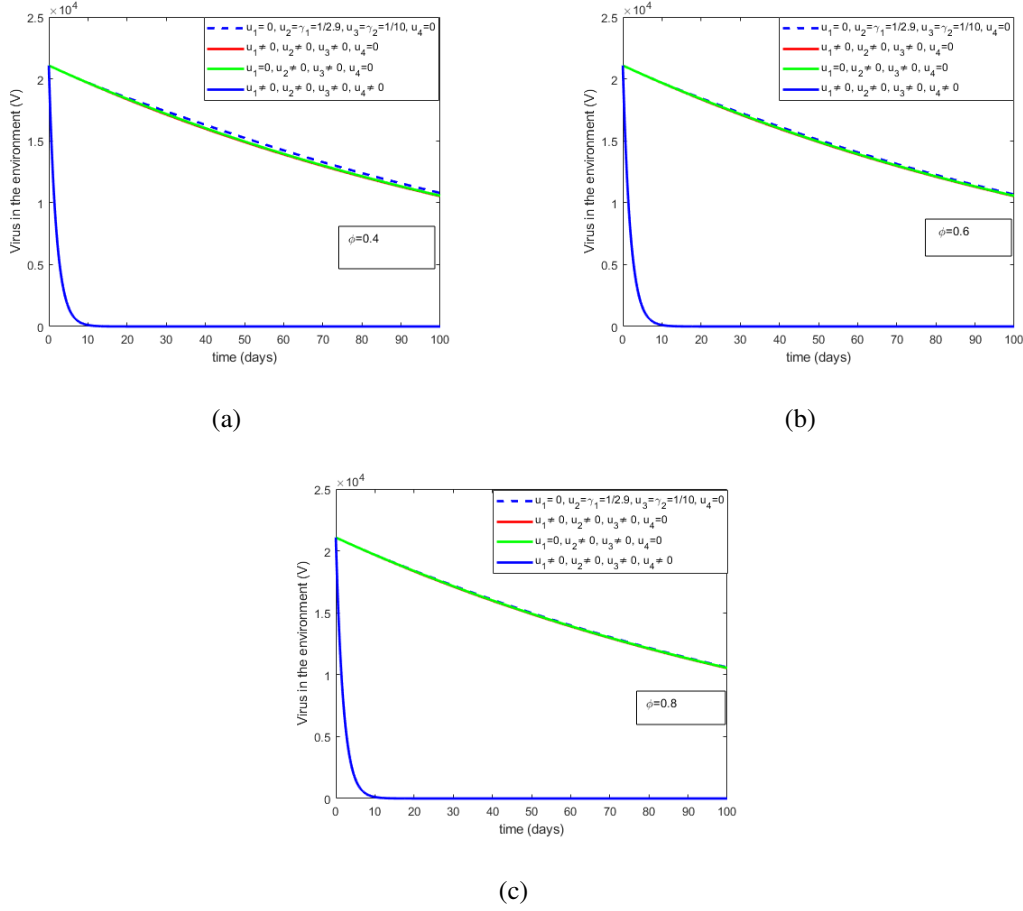
FIGURE 14. Solutions trajectories for virus in the environment with $\phi = 0.4$, $\phi = 0.6$ and $\phi = 0.8$.

4. CONCLUSION

In this study, we have formulated and studied a new optimal control dynamical model for the 2019 coronavirus disease. Our new non-autonomous mathematical model for the 2019 coronavirus disease, which is characterised by a system of nonlinear ordinary differential equations, is an extension of a recently constructed and analyzed data-driven non-optimal control model studied [16]. We have presented three control strategies to examine the dynamics of COVID-19 deadly infectious disease. We incorporated four optimal time-dependent control functions into the nonlinear dynamical optimal control problem. These control functions included personal protection, hospitalization and treatment with early diagnosis, hospitalization and treatment

with delayed diagnosis and spraying of the environment, and cleaning possible infected surfaces. The numerical simulations reveal that optimal control strategies can yield a significant reduction in the number of COVID-19 exposed and infectious or infected individuals in the population. By instituting control strategies, we realized that the number of days required for the virus to be eliminated from the system is significantly reduced as compared to when there is no control strategy. The numerical illustrations also show that by increasing ϕ i.e. improving the diagnostic resources, and increasing γ_2 i.e. improving the diagnostic efficiency, we can control significantly the number of new confirmed cases, new infections and thus can reduce the transmission risk. From all the three control strategies considered in this study, we realized that the third strategy, which captures all the four time-dependent control functions, yields better results.

Conflict of Interests

The author(s) declare that there is no conflict of interests.

References

[1] World Health Organization, WHO Director-General's opening remarks at the media briefing on COVID-19 - 11 March 2020, 2020. https://www.who.int/dg/speeches/detail/who-director-general-s-opening-remarks-at-the-media-briefing-on-covid-19—11-march-2020.

[2] World Health Organization, Coronavirus disease (COVID-19) weekly epidemiological update and weekly operational update, 2020.
https://www.who.int/emergencies/diseases/novel-coronavirus-2019/situation-reports.

[3] C. Young, Covid-19: Novel Coronavirus Content Free to Access, John Wiley & Sons, Hoboken, New Jersey, 2020, https://novel-coronavirus.onlinelibrary.wiley.com/.

[4] Wiley, Covid-19 resources, 2020. https://www.wiley.com/network/covid-19-resources.

[5] Elsevier, Novel coronavirus information center, 2020.
https://www.elsevier.com/connect/coronavirus-information-center.

[6] Hindawi, Covid-19 collection: Sars-cov-2 and covid-19, 2020.
https://www.hindawi.com/covid-19-collection.

[7] Springer Nature, Coronavirus (COVID-19) research highlights, 2020.
https://www.springernature.com/gp/researchers/campaigns/coronavirus.

[8] F. Brauer, Mathematical epidemiology: Past, present, and future, Infect. Dis. Model. 2 (2017), 113–127.

[9] C.I. Siettos, L. Russo, Mathematical modeling of infectious disease dynamics, Virulence, 4 (2013), 295-306.

[10] H.W. Hethcote, The mathematics of infectious diseases, SIAM Rev. 42 (2000), 599–653.

[11] A. Zeb, E. Alzahrani, V.S. Erturk, G. Zaman, Mathematical model for coronavirus disease 2019 (COVID-19) containing isolation class, BioMed Res. Int. 2020 (2020), 3452402.

[12] T. Götz, P. Heidrich, Early stage COVID-19 disease dynamics in Germany: models and parameter identification, J. Math. Ind. 10 (2020), 20.

[13] J. Wangping, H. Ke, S. Yang, et al. Extended SIR prediction of the epidemics trend of COVID-19 in Italy and compared with Hunan, China, Front. Med. 7 (2020), 169.

[14] M. Mandal, S. Jana, S.K. Nandi, A. Khatua, S. Adak, T.K. Kar, A model based study on the dynamics of COVID-19: Prediction and control, Chaos Solitons Fractals. 136 (2020), 109889.

[15] Y. Fang, Y. Nie, M. Penny, Transmission dynamics of the COVID-19 outbreak and effectiveness of government interventions: A data-driven analysis, J. Med. Virol. 92 (2020), 645–659.

[16] X. Rong, L. Yang, H. Chu, M. Fan, Effect of delay in diagnosis on transmission of COVID-19, Math. Biosci. Eng. 17 (2020), 2725–2740.

[17] K. Mizumoto, G. Chowell, Estimating risk for death from coronavirus disease, China, January–February 2020, Emerg. Infect. Dis. 26 (2020), 1251–1256.

[18] K. Roosa, Y. Lee, R. Luo, A. Kirpich, R. Rothenberg, J.M. Hyman, P. Yan, G. Chowell, Real-time forecasts of the COVID-19 epidemic in China from February 5th to February 24th, 2020, Infect. Dis. Model. 5 (2020), 256–263.

[19] Q. Lin, S. Zhao, D. Gao, et al. A conceptual model for the coronavirus disease 2019 (COVID-19) outbreak in Wuhan, China with individual reaction and governmental action, Int. J. Infect. Dis. 93 (2020), 211–216.

[20] S. Annas, Muh. Isbar Pratama, Muh. Rifandi, W. Sanusi, S. Side, Stability analysis and numerical simulation of SEIR model for pandemic COVID-19 spread in Indonesia, Chaos Solitons Fractals. 139 (2020), 110072.

[21] B. Buonomo, Effects of information-dependent vaccination behavior on coronavirus outbreak: insights from a SIRI model, Ricerche Mat. 69 (2020), 483–499.

[22] A. Abou-Ismail, Compartmental models of the COVID-19 pandemic for physicians and physician-scientists, SN Compr. Clin. Med. 2 (2020), 852–858.

[23] G. Rohith, K.B. Devika, Dynamics and control of COVID-19 pandemic with nonlinear incidence rates, Nonlinear Dyn. 101 (2020), 2013–2026.

[24] S. Mushayabasa, E.T. Ngarakana-Gwasira, J. Mushanyu, On the role of governmental action and individual reaction on COVID-19 dynamics in South Africa: A mathematical modelling study, Inform. Med. Unlocked. 20 (2020), 100387.

[25] M. Ali, S.T.H. Shah, M. Imran, A. Khan, The role of asymptomatic class, quarantine and isolation in the transmission of COVID-19, J. Biol. Dyn. 14 (2020), 389–408.

[26] S. He, Y. Peng, K. Sun, SEIR modeling of the COVID-19 and its dynamics, Nonlinear Dyn. 101 (2020), 1667–1680.

[27] S. Lenhart, J.T. Workman, Optimal control applied to biological models, Chapman and Hall/CRC, 2007.

[28] O. Sharomi, T. Malik, Optimal control in epidemiology, Ann Oper Res. 251 (2017), 55–71.

[29] M. Stehlík, J. Kiseľák, M.A. Dinamarca, Y. Li, Y. Ying, On COVID-19 outbreaks predictions: Issues on stability, parameter sensitivity, and precision, Stoch. Anal. Appl. 39 (2021), 383–404.

[30] A.A. Momoh, A. Fügenschuh, Optimal control of intervention strategies and cost effectiveness analysis for a Zika virus model, Oper. Res. Health Care. 18 (2018), 99–111.

[31] E. Okyere, J. De-Graft Ankamah, A.K. Hunkpe, D. Mensah, Deterministic epidemic models for ebola infection with time-dependent controls, Discr. Dyn. Nat. Soc. 2020 (2020), 2823816.

[32] E. Bonyah, M.A. Khan, K.O. Okosun, J.F. Gómez-Aguilar, Modelling the effects of heavy alcohol consumption on the transmission dynamics of gonorrhea with optimal control, Math. Biosci. 309 (2019), 1–11.

[33] H.W. Berhe, O.D. Makinde, Computational modelling and optimal control of measles epidemic in human population, Biosystems. 190 (2020), 104102.

[34] L.S. Pontryagin, The mathematical theory of optimal processes and differential games, Trudy Mat. Inst. Steklov, 169 (1985), 119–158.

[35] L.S. Pontryagin, V.G. Boltyanskii, R.V. Gamkrelidze, E.F. Mishchenko, The mathematical theory of optimal processes, Wiley, New York, 1962.

[36] W.H. Fleming, R.W. Rishel, Deterministic and stochastic optimal control, Stochastic modelling and applied probability, Springer, New York, 2012.

[37] A. Hugo, O.D. Makinde, S. Kumar, F.F. Chibwana, Optimal control and cost effectiveness analysis for Newcastle disease eco-epidemiological model in Tanzania, J. Biol. Dyn. 11 (2017), 190–209.

[38] R.L. Miller Neilan, E. Schaefer, H. Gaff, K.R. Fister, S. Lenhart, Modeling optimal intervention strategies for cholera, Bull. Math. Biol. 72 (2010), 2004–2018.

[39] K.O. Okosun, O.D. Makinde, A co-infection model of malaria and cholera diseases with optimal control, Math. Biosci. 258 (2014), 19–32.